A mechanical model of vocal-fold collision with high spatial and temporal resolution[a)]

Heather E. Gunter[b)]
Division of Engineering and Applied Sciences, Harvard University, Pierce Hall, 29 Oxford Street, Cambridge, Massachusetts 02138

(Received 18 April 2002; accepted for publication 1 November 2002)

The tissue mechanics governing vocal-fold closure and collision during phonation are modeled in order to evaluate the role of elastic forces in glottal closure and in the development of stresses that may be a risk factor for pathology development. The model is a nonlinear dynamic contact problem that incorporates a three-dimensional, linear elastic, finite-element representation of a single vocal fold, a rigid midline surface, and quasistatic air pressure boundary conditions. Qualitative behavior of the model agrees with observations of glottal closure during normal voice production. The predicted relationship between subglottal pressure and peak collision force agrees with published experimental measurements. Accurate predictions of tissue dynamics during collision suggest that elastic forces play an important role during glottal closure and are an important determinant of aerodynamic variables that are associated with voice quality. Model predictions of contact force between the vocal folds are directly proportional to compressive stress ($r^2=0.79$), vertical shear stress ($r^2=0.69$), and Von Mises stress ($r^2=0.83$) in the tissue. These results guide the interpretation of experimental measurements by relating them to a quantity that is important in tissue damage. © *2003 Acoustical Society of America.* [DOI: 10.1121/1.1534100]

PACS numbers: 43.70.Aj, 43.70.Jt, 43.70.Bk [AL]

I. INTRODUCTION

Vocal-fold biomechanics play an important role in voice production. In particular, the solid mechanics underlying collision between the vocal folds are interesting due to their association with aerodynamic variables that are linked to voice quality changes (Holmberg *et al.*, 1988), and their proposed role in increasing mechanical stress levels that may cause tissue damage (Titze, 1994). A detailed theoretical model of vocal-fold tissue mechanics during collision that connects tissue-damaging variables with clinical/experimental variables and vice versa is an excellent tool with which to clarify the impact stress hypothesis. It also has the potential to predict the effect of surgical manipulation of vocal-fold structure on voice quality.

The impact stress hypothesis of vocal nodule development assumes that forces applied to the medial vocal fold during collision correlate with mechanical stresses in superficial tissue. Situations that increase collision force are thought to increase the risk of tissue damage and pathology development by increasing mechanical stresses levels (Titze, 1994). The stresses that are likely to be associated with collision and cause tissue damage include compressive stress perpendicular to the plane of contact that may cause cellular rupture and shear stress parallel to the plane of contact that may cause separation of tissue elements. Damage may also be caused by alterations in cellular function in response to the stress environment. The environment can be quantified by Von Mises stress, a scalar stress quantity that is used in engineering to represent composite stress in a material (Chandrupatla and Belegundu, 1997). The pathologies observed are 1–2 mm in size and involve the thickness of the lamina propria (Dikkers, 1994). Therefore, it is likely that mechanical stress changes occur on a similar or smaller scale. Jiang and Titze (1994) and Hess *et al.* (1998) cite the impact stress hypothesis as their motivation for identifying situations that increase intrafold collision forces and implying corresponding increases in mechanical stresses. The relationship between measured total collision forces and distributed mechanical stresses remains to be defined.

A theoretical model of vocal-fold collision that captures the dynamics of vocal-fold closure has the potential to be applied to prediction of the surgical outcomes. This would address the subset of vocal-fold surgeries where vocal-fold structure is manipulated in order to improve voice quality (Zeitels, 1998). Surgical manipulation of individual layers of vocal-fold tissue alters tissue vibration, which affects the glottal aerodynamic waveform and the acoustic voice spectrum. Voice quality is linked to changes in the aerodynamic variables maximum flow declination rate and minimum flow (Holmberg *et al.*, 1988). Vocal-fold closure and collision are the tissue correlates of these variables.

The idea to represent vocal-fold tissue mechanics mathematically is not a new one. Lumped mass models of phonation with as few as two (Ishizaka and Flanagan, 1972) or three (Story and Titze, 1995), and as many as 16 (Titze, 1973, 1974) masses predict aerodynamic and acoustic waveforms. Collision is represented by a spring that becomes active as a mass crosses the glottal midline. Story and Titze predict intraglottal collision pressures that agree qualitatively with Jiang and Titze's (1994) experimental measurements. However, the theoretical peak pressure prediction is approxi-

[a)]Portions of this work were presented in "Analysis of Factors Affecting Vocal Fold Impact Stress Using a Mechanical Model," 142nd meeting of the Acoustical Society of America, Ft. Lauderdale, FL, December 2001.
[b)]Electronic mail: gunter@fas.harvard.edu

mately fivefold less than the comparable experimental measurement (Jiang and Titze, 1994). The spatial resolution of the lumped mass models is insufficient to reflect the scale of pathology and surgery, and their empirically assigned spring, damper, and mass values have few direct implications for vocal-fold tissue physiology. Analytical continuum mechanics approaches (Titze and Strong, 1975; Berry and Titze, 1996) permit infinite spatial resolution but require simplified geometries (i.e., rectangular prisms) that make representation of pathological and surgical alterations difficult.

Alipour *et al.*'s (1996, 2000) and Jiang *et al.*'s (1998) models of phonation use finite-element techniques that overcome the barriers of low spatial resolution and restricted geometries. These techniques involve spatially and temporally discretizing a continuum mechanics problem into solid elements and time increments followed by numerical solution. Alipour *et al.*'s (2000) self-oscillating model requires increased spatial resolution, calculation of mechanical stress distributions, and extension to true three-dimensionality in order to represent vocal-fold pathologies and examine mechanical stress distributions. Jiang *et al.*'s (1998) finite-element model of vocal-fold tissue has sufficient spatial resolution to represent pathology, but limits analysis to resonant and forced vibration. It requires an explicit representation of collision forces between the vocal folds in order to be used in investigations of contact related pathology etiologies and voice quality.

A finite-element model of vocal-fold collision that is not self-oscillating is presented below. It has spatial resolution that is capable of representing the submillimeter scale of vocal-fold injury and repair, temporal resolution that captures the submillisecond time scale of vocal-fold collision, and an explicit representation of vocal-fold collision. Model predictions of collision force are validated against experimental data and the model potential is illustrated in an examination of the relationships between collision force and mechanical stress levels.

II. DEVELOPMENT

A. Assumptions

The model of vocal-fold collision presented below has three unique features. The spatial resolution of 250 μm is finer than that incorporated in other vocal-fold models. A single isotropic, linear elastic material characterizes the entire vocal-fold structure. Glottal closure during phonation is represented using a nonoscillating model consisting of appropriate initial conditions and a high-fidelity model of vocal-fold solid mechanics. Justifications for these features are outlined below.

The necessary spatial resolution is dictated by the size of geometric variations in the model, the desired resolution of model outputs, and desired computational speed. The model is intended for use in studying the effects of vocal-fold pathologies and their repair on tissue movement and for investigating the distribution of mechanical stresses in vocal-fold tissue as an indication of pathology development risk. Benign vocal-fold pathologies such as nodules and polyps have dimensions of 1–2 mm on the vocal-fold surface (Dikkers, 1994). Spanning the pathology with a minimum of four elements requires element dimensions of 250 μm and allows for some sculpting of the geometry. Surgical repair of the vocal fold can involve manipulation of only the superficial lamina propria (Zeitels, 1998), which, at approximately 500 μm thick (Hirano *et al.*, 1983), can be represented by two elements. Mechanical stresses that are important in tissue injury are on the same scale as or smaller scale than the pathologies that they are proposed to cause. Therefore, a resolution that is sufficient to represent pathologies provides appropriate information on stress distributions. Further resolution would increase geometric fidelity and output detail, but would also increase computational load significantly.

A simple material definition is used in the model. The assumption of linear elasticity is consistent with Min *et al.*'s (1995) observation of linear stress–strain behavior of human vocal ligaments for strains of less than 15%. Strains in the model do not exceed this 15% upper bound. The primary mode of deformation of the vocal fold during vocal-fold closure is compressive in the transverse (i.e., medial–lateral and inferior–superior) directions. Due to the lack of direct data on the elastic properties of vocal-fold tissue when undergoing this kind of deformation, isotropy is assumed and elastic properties based on longitudinal (i.e., anterior–posterior) tensile deformation are used for guidance. The range of elastic moduli derived by Min *et al.* (1995) using human vocal ligament samples (21.2–42.2 kPa) spans the moduli derived by Alipour-Haghighi and Titze (1991) for unstimulated canine thyroarytenoid muscle (20.7 kPa) and canine vocal-fold cover (41.1 kPa) and are the same order of magnitude as moduli derived by Kakita *et al.* (1981) using canine vocal-fold muscle and cover. The assumption of homogeneous properties is within the spread of the data in the literature.

Some studies suggest that air pressure in the glottis is low during glottal closure. The myoelastic-aerodynamic theory of voice production cites three reasons for glottal closure: elastic recoil of the deformed tissue, decreased pressure on the glottal walls due to the high velocity of the air stream through the opening, and decreased subglottal pressure (Jiang *et al.*, 2000). Experimental measurements performed on canine hemilarynges illustrate that, in an almost fully adducted larynx, air pressure in the glottis remains below 10% of subglottal pressure during glottal closure, and does not rise until full closure has occurred (Alipour and Scherer, 2000). Measurements performed on excised human hemilarynges also demonstrate reduced glottal air pressures during closure (Alipour *et al.*, 2001). It is consistent with observations of minimum air pressures and maximum vocal-fold deformation when the glottis is fully open to postulate that elastic forces dominate during glottal closure, and to focus on these forces in a model of glottal closure.

B. Implementation

The model geometry shown in Fig. 1 represents the membranous portion of a fully adducted single vocal fold. The model is defined in Cartesian coordinates. The origin is middle of the posterior glottis, inferior to the bulge of the vocal fold. The y axis defines the midline of the glottis, x dimensions indicate lateral distance from the glottal midline,

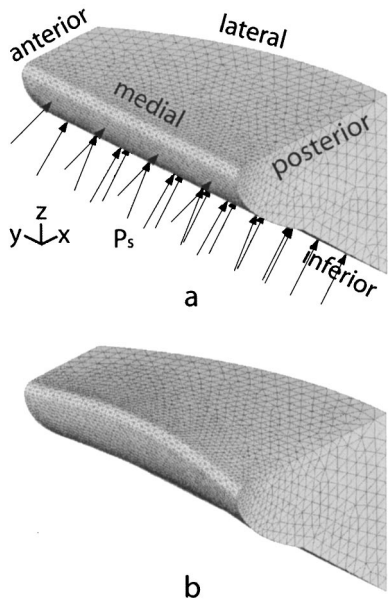

FIG. 1. Calculation of initial conditions for glottal closure using a finite-element model of the vocal fold. (a) problem formation: the three-dimensional solid represents the undeformed vocal fold. Triangular divisions indicate individual three-dimensional finite elements. Anterior, lateral, and posterior boundaries are held fixed. The arrows indicate the direction and location of application of forces representing subglottal pressure (P_s). (b) Problem solution: the three-dimensional solid represents the deformed vocal fold. This output is dependent on subglottal pressure and is the initial condition for glottal closure (see Fig. 2).

and z translations represent movement in the vertical direction. The vocal-fold dimensions are 1.4 cm long (y direction), 0.5 cm wide anteriorly, 1.0 cm wide posteriorly (x direction), and 1.0 cm high posteriorly (z direction). The anterior, posterior, and lateral surfaces are fixed to represent their attachment to the laryngeal cartilages. This structure is based on Titze and Talkin (1979) and uses their nominal parameters [i.e., shaping factor (s) equal to 0.05 radians, glottal angle (w) equal to 0.0 radians, and inferior surface angle (q) equal to 0.7 radians]. The Titze and Talkin geometry is modified by applying a fillet with a radius of 0.05 cm to the superior medial curve in order to create a smooth contour in the coronal plane. The glottal width (g) between the inferior aspect of the fillet and the superior aspect of the inferior surface is derived from an expression given by Titze and Talkin

$$g(0.05 \leqslant h \leqslant 0.5) = 0.45 - 1.9(h - 0.5) + 2(h - 0.5)^2,$$

where h is the vertical distance below the superior surface. The minimum glottal width of 0.0 cm that occurs at the inferior end of the fillet (h equal to 0.05 cm) indicates that the undeformed vocal fold is tangent to the glottal midline. A similar geometry has been used by Alipour *et al.* (2000) with good results.

A finite-element support software package (FEMAP 8.0; EDS, Inc., Plano, TX) is used to divide the geometry into 14 242 three-dimensional tetrahedral elements, which provides an elemental resolution of 250 μm on the medial surface. The model has 23 637 nodes, which reflect the ten nodes necessary to define each element and provide 70 911 degrees of freedom. Repetition of analyses using a model with 2.5-fold fewer elements affects collision force predictions by a maximum of 4%, which indicates that the mesh is fine enough to achieve convergence of results.

A common material defines all elements in the model. The material properties are nondirectional and linear, with a Young's modulus (E) of 36.1 kPa and a Poisson's ratio (ν) of 0.3. These parameters are based on experimental measurements on human vocal ligament samples by Min *et al.* (1995) and are valid for strains of less than 15%. None of the simulations presented below produces strains greater than this magnitude. The first mode of vibration is calculated using a linear perturbation eigenvalue analysis of the vocal-fold geometry in the absence of the pressure load and contact condition (ABAQUS STANDARD 5.8.1; HKS Inc.; Pawtucket, RI) to provide an evaluation of the geometric and material representations.

Interaction between the vocal fold and a rigid surface in the middle of the glottis (i.e., a yz plane at $x=0$, shown as thick black lines in Fig. 2) represents the interaction between the modeled fold and the opposing vocal fold. This surface and the nodes on the medial surface of the vocal fold form a contact pair: As a medial surface node becomes coincident with the rigid surface, sufficient force is applied to prevent the node from passing through the surface. Contact forces are in the x direction since the interaction is frictionless. Total contact force is the sum of the forces acting on all medial surface nodes. Contact area is a function of the number of nodes that are in contact with the surface. When the vocal fold it in its neutral position the contact area is 7 mm^2.

Deformation of the vocal-fold model due to subglottal pressure (P_s) defines the initial condition for vocal-fold closure. A distributed load applied perpendicularly to the element faces that form the inferior and medial surfaces as shown in Fig. 1(a) represents subglottal pressure. Equilibrium tissue deformation [Figs. 1(b), 2(a)] and stress distributions [Fig. 2(a)], calculated for each subglottal pressure ($P_s = 0.4$, 0.6, 0.8, 1.0, 1.5, and 2.0 kPa) (ABAQUS STANDARD 5.8-1), define the maximally open glottis. Geometric nonlinearities are accounted for during this calculation.

Vocal-fold closure is the progression from maximally open [Fig. 2(a)] to fully closed [Fig. 2(c)] glottis due to elastic forces within the tissue. The nonlinear, transient, dynamic solution for a given initial condition is obtained by incrementing forward through time using implicit integration algorithms (ABAQUS STANDARD 5.8-1). Time increments that result in solution convergence, calculated based on the half-step residual and changes in the contact state, range from 10–100 μs before collision occurs and 10–100 ps during collision. Typically between 50 and 100 increments are necessary to predict 3 ms of tissue movement and capture complete vocal-fold closure. Outputs of these calculations include movement of each node, mechanical stresses in each element, and interactions between nodes and the rigid midline surface.

The goals with this model are to validate predictions of closure kinematics and collision surface forces against published experimental measurements, and to examine the relationship between collision surface forces and mechanical stress levels in the tissue during collision. Model predictions that reflect these goals are discussed below.

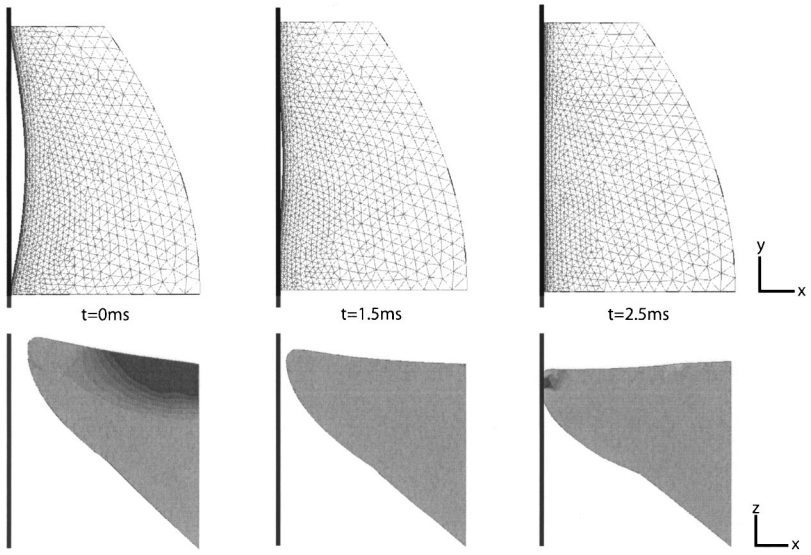

FIG. 2. Finite-element model of the membranous portion of a vocal fold during glottal closure. Each column provides two views of the model at one time increment. The vertical lines represent the plane of contact with the opposing vocal fold. Images in the top row are superior views, similar to those obtained clinically using a laryngoscope, that illustrate the changing glottal area. The bottom row of images are coronal sections through the midmembranous region of the vocal fold. The degree of dark shading in the bottom row of images represents the magnitude of compressive stress in the tissue in the direction perpendicular to the plane of contact. The images in the left-hand column represent the initial condition. The deformation is due to the application of a subglottal pressure of 2 kPa. There are compressive stresses in the superior lateral region with a maximum magnitude of 3.5 kPa. This provides the elastic energy that causes the fold to move. The middle and right-hand columns show frames in the solution. The images in the middle column represent the deformation of the vocal fold 1.5 ms after the start of glottal closure. There are no compressive stresses greater than 3 kPa. The images in the right-hand column represent the deformation of the vocal fold 2.5 ms after the start of glottal closure. There is a compressive stress concentration with a magnitude of 10 kPa at the site of contact with the opposing fold.

III. VALIDATION

The natural frequency is 127 Hz, which is consistent with experimentally measured resonant frequencies (Kaneko *et al.*, 1987) and theoretically predicted resonant frequencies for adult male voices (Alipour *et al.*, 2000). This agreement corroborates the geometric and material definitions.

Glottal closure dynamics are an important output of the model, and model behavior agrees with observations of vocal-fold vibration. The qualitative movement of the fold shown in Fig. 2 includes movement towards the midline and collision with the opposing fold. Closure begins at the anterior and posterior ends and progresses towards the midmembranous region (Fig. 2, top row), which is consistent with *in vivo* stroboscopic observations of fully adducted phonation. The initial midmembranous glottal displacement (i.e., the maximum lateral displacement of the medial vocal-fold edge) is an approximately linear function of subglottal pressure and ranges between 0.15 and 0.8 mm as illustrated in Fig. 3. These predictions are consistent with previous visual observations of normal vocal-fold vibration (Zemlin, 1998). The inferior portion of the vocal-fold edge is the first point of collision with the opposing fold. As collision proceeds, contact includes the superior vocal-fold edge (Fig. 2, bottom row). This progression is similar to phase differences that are observed clinically. Contact areas, which are calculated based on the number of elements touching the midline surface in the step 2 solutions, are also functions of P_s and time, as shown in Fig. 4. The contact areas range from 0 to 13 mm^2, which lies within the area of vocal-fold contact imaged by Jiang and Titze (1994).

Collision dynamics during closure are another important output of the model, and model behavior agrees with published experimental results. As shown in Fig. 5, the total collision force increases with time and reaches either a peak or a plateau depending on the initial P_s. The rise time of collision in a 3-mm midmembranous region for $P_s = 1.5$ and 2.0 kPa is approximately 0.5 ms, which is equal to the experimentally measured rise time for impact with a 3-mm diameter central sensor as measured in canine hemilarynges by Jiang and Titze (1994). Due to the collision force plateau, there are no clear force peaks for P_s less than 1.5 kPa. Collision force peaks are defined either as the force magnitude at

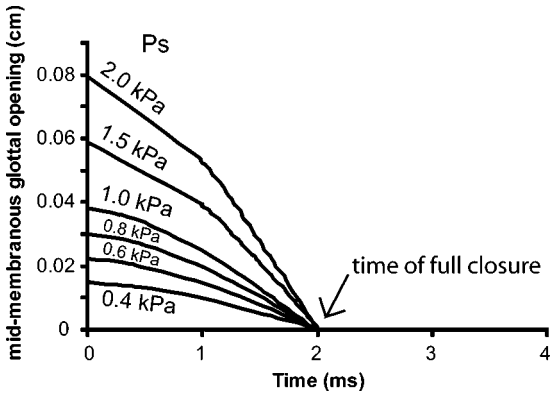

FIG. 3. Effect of subglottal pressure on the medial movement of the vocal fold—Each line traces the solution for the x position of a midmembranous point on the medial edge of the vocal-fold edge during glottal closure in a single model. The models differ by the subglottal pressure magnitude used to calculate the initial closure condition (i.e., $t = 0$). The arrow points to the time when the midmembranous glottal opening and glottal area are zero, which is defined as the time of full closure. This value is not dependent on subglottal pressure.

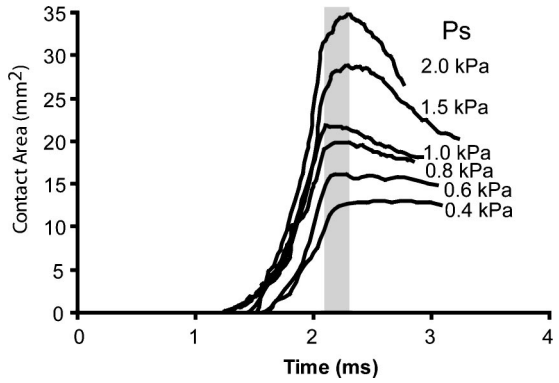

FIG. 4. Effect of subglottal pressure on the area of contact between the vocal fold and the contact surface—Each line traces the solution for contact area, which is proportional to the number of nodes that are at $x=0$ (i.e., touching the contact plane) during glottal closure in a single model. The models differ by the subglottal pressure used to calculate the initial condition of glottal closure (i.e., $t=0$). The shaded area indicates the temporal range of contact area maxima, which varies among models.

the time of full closure, which is independent of P_s as shown in Fig. 3, or as the force magnitude at the time of maximum contact area, which is dependent on P_s as shown in Fig. 4. These peaks are used to derive linear relationships between subglottal pressure and peak collision force. Table I compares the slopes and regression coefficients for linear best-fit lines derived from model predictions with data derived from *in vitro* experiments on canine hemilarynges by Jiang and Titze (1994). Both definitions of predicted peak collision force fall within the span of the experimental results.

IV. MECHANICAL STRESS DURING COLLISION

To determine whether local collision force predicts local mechanical stress, a regression analysis between contact force predictions and mechanical stress predictions is performed. For each time point during vocal-fold collision and at each 1-mm interval along the vocal-fold edge, contact force and medial superficial stresses are extracted from model results. Compressive stress perpendicular to the plane of contact, shear stress parallel to the plane of contact in the

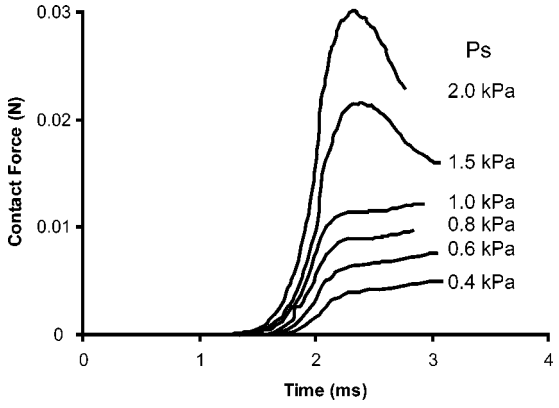

FIG. 5. Effect of subglottal pressure on the total contact force between the vocal fold and the contact surface. Each line traces the solution for contact force, which is the sum of point loads applied by the contact plane to nodes on the medial surface, during glottal closure in a single model. The models differ by the subglottal pressure magnitude used to calculate the initial condition of glottal closure (i.e., $t=0$).

TABLE I. Comparison between linear regression analysis of peak contact force and subglottal pressure for theoretical predictions using a finite-element model and Jiang and Titze's (1994) experimental measurements on canine hemilarynges.

Contact force definition	Linear slope (mN/kPa)	Regression coefficient
Model prediction—peak contact area	16.39	0.977
Model prediction—full closure	10.48	0.930
Experimental measurement (Jiang and Titze, 1994)	Range=7.70–26.60 Mean=12.46	

longitudinal direction, shear stress parallel to the plane of contact in the vertical direction, and Von Mises stress are examined. Figure 6 shows the relationship between contact force and stresses for a subglottal pressure of 1 kPa. At this subglottal pressure there is a general trend between increases in local contact force and increases in compressive stress ($r^2=0.79$), vertical shear stress ($r^2=0.69$), and Von Mises stress ($r^2=0.83$). There is no trend between local contact force and longitudinal shear stress ($r^2=0.00$). Local variations from the general trends can be appreciated by examining the data points for each 1-mm segment. The variations are most pronounced for longitudinal shear stress, where there are local inverse trends between contact force and stress despite the lack of a general trend.

V. DISCUSSION

This model examines the time and spatial course of vocal-fold closure, but not separation, during phonation and makes two contributions. The first contribution is accurate prediction of closure kinematics and collision surface forces, despite the absence of an aerodynamic representation and an assumption of homogeneous material properties. This provides insight as to the importance of elastic forces in glottal closure and supports future application to the study of the effects of vocal-fold tissue elasticity and structure on the dynamics of glottal closure, corresponding aerodynamic variables, and, by extension, voice quality.

The second contribution is an illustration of the potential of this model of glottal closure to provide a window to mechanical conditions in the vocal-fold interior that may increase injury risk. Regressions between surface contact force and relative predictions of mechanical stress in the tissue indicate that the implications of experimental impact force measurements are position dependent and identify compressive stress perpendicular to the contact plane, shear stress parallel to the contact plane in the longitudinal direction, and Von Mises stress as candidate mechanical stresses that may cause tissue damage as a result of high collision forces.

The ability of this model to predict closure kinematics and collision surface forces despite exclusion of aerodynamic forces from the model provides insight into the mechanics of voice production. Agreements between model predictions and published data suggest that elastic forces within the tissue dominate the mechanics of vocal-fold closure and collision, and are therefore a major determinant of aerodynamic variables that are associated with closure, such as minimum flow and maximum flow declination rate (MFDR).

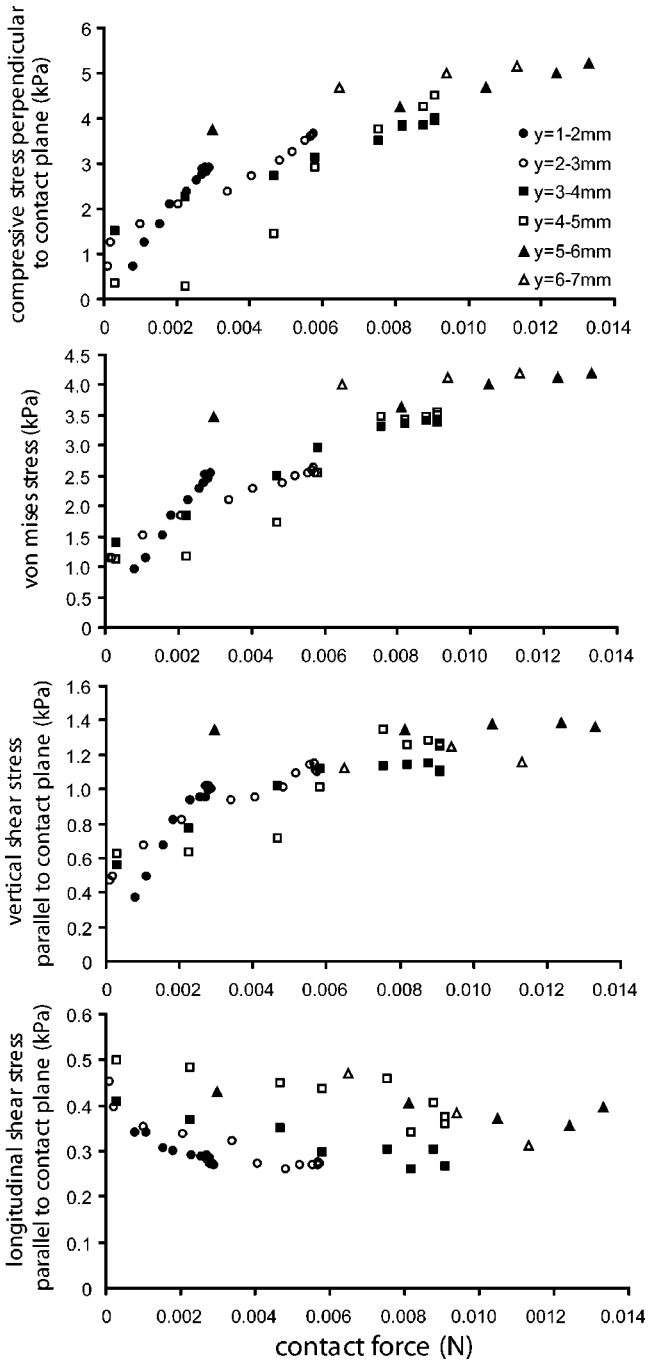

FIG. 6. Relationship between local contact force and mechanical stress on the medial vocal-fold surface during collision. The x value of each data point represents the integrated contact force over a 1-mm vertical slice of the medial surface. The y value of each data point represents the maximum mechanical stress in the surface tissue in the same 1-mm slice. Data are symmetric about the midmembranous location ($y=7$ mm). For simplicity, only data for the anterior half of the fold are shown. Correlation coefficients are given in the text.

The dependence of voice quality on MFDR and minimum flow allows extension of this hypothesis to propose that solid mechanics of vocal-fold tissue are a dominant factor in voice quality. *In vivo* associations between structural changes that affect vocal-fold closure, such as vocal nodules, increased minimum flow, decreased MFDR, and altered voice quality perceptions (Kuo, 1998) support this hypothesis.

The suggestion that tissue mechanics dominate vocal-fold closure kinematics, important aerodynamic variables, and voice quality reinforces the proposed use of a vocal-fold collision model to predict surgical outcomes. Comparison of the closure dynamics between models of vocal folds with organic pathologies and models of the same folds following surgical repair will allow prediction of the effects of surgery on voice quality. The prognostic value of this application may be further refined by incorporation of a layered geometrical structure and more complex material property definitions; these will facilitate the creation of higher fidelity models of pathology and surgical changes.

The lack of a defined contact force peak in models with low subglottal pressures and the lack of a reopening phase in all models does not agree with clinical observations of glottal opening, but was not an intended focus of this model. These results indicate that bouncing of the vocal folds following collision is not sufficient to cause glottal opening and reinforces the important role played by air pressure in vocal-fold separation. Comparison of the current results with those from a new model with a sophisticated aerodynamic representation will test the hypothesis that tissue elasticity forces dominate during glottal closure and that aerodynamic forces dominate during vocal-fold separation.

Agreement between model glottal closure kinematics and collision surface forces and experimental measurements does not necessarily imply that model predictions of mechanical stress are accurate. It is the case, in any complex model with multiple input variables, that there may not be one unique combination that produces the desired output. In the case of this model, prediction of appropriate contact surface forces and closure kinematics only implies that one appropriate set of input parameters was identified. A different combination of input parameters may have provided the same surface contact force predictions, but different absolute mechanical stress predictions. However, it is likely that the relative nature of mechanical stress predictions would remain the same. Therefore, it is reasonable to compare them against each other.

The relationships between contact forces on the vocal-fold surface and superficial tissue mechanical stress in the medial edge of the vocal fold, derived using a model of vocal-fold collision, guide the interpretation of experimental contact force measurements. Local collision force measurements are indicative of local compressive stress, vertical shear stress, and Von Mises stress. This observation suggests that pathologies associated with maneuvers that have increased local impact forces (e.g., phonation with high subglottal pressures) may be due to a compressive mode of tissue failure, a shear mode of tissue failure, or alterations in cellular behavior. Unfortunately, without knowledge of what stress magnitudes cause tissue failure, it is impossible to comment on which stress levels are most damaging to the tissue. Correlations between stress predictions and epidemiology of lesions that reflect tissue injury, such as vocal nodules, will test the impact stress hypothesis of pathology development.

Additional experimental measurements will improve definition and validation of the vocal-fold collision model and other models of vocal-fold tissue mechanics. Three-

dimensional material property data based on human vocal-fold tissue samples undergoing compression would improve the fidelity of model inputs. *In vivo* human results of surface collision forces would be a preferred source against which to validate model predictions because agreement will enhance the applicability of the model to human voice. Other experimental measurements that will be useful in validation include electroglottographic measurements of contact area and photoglottographic measurements of glottal area.

ACKNOWLEDGMENTS

Thank you to Ken Stevens, Robert Hillman, and Robert Howe for their scientific guidance and assistance with manuscript preparation, to Jaime Lee for her assistance with data analysis, to the J. Acoust. Soc. Am. reviewers and editors for their valuable feedback, and to the Whitaker Foundation for financing this work through a Biomedical Engineering Graduate Fellowship.

Alipour, F., Berry, D. A., and Titze, I. R. (**2000**). ''A finite-element model of vocal-fold vibration,'' J. Acoust. Soc. Am. **108**, 3003–3012.

Alipour, F., Montequin, D., and Tayama, N. (**2001**). ''Aerodynamic profiles of a hemilarynx with a vocal tract,'' Ann. Otol. Rhinol. Laryngol. **110**, 550–555.

Alipour, F., and Scherer, R. C. (**2000**). ''Dynamic glottal pressures in an excised hemilarynx model,'' J. Voice **14**, 443–54.

Alipour, F., and Titze, I. R. (**1996**). ''Combined simulation of two-dimensional airflow and vocal fold vibration,'' in *Vocal Fold Physiology: Controlling Complexity and Chaos*, edited by P. J. Davis and N. H. Fletcher (Singular, San Diego), pp. 17–30.

Alipour-Haghighi, F., and Titze, I. R. (**1991**). ''Elastic models of vocal fold tissues,'' J. Acoust. Soc. Am. **90**, 1326–1331.

Berry, D. A., and Titze, I. R. (**1996**). ''Normal modes in a continuum model of vocal fold tissues,'' J. Acoust. Soc. Am. **100**, 3345–3354.

Chandrupatla, T. R., and Belegundu, A. D. (**1997**). *Introduction to Finite Elements in Engineering*, 2nd ed. (Prentice-Hall, Englewood Cliffs, NJ), p. 17.

Dikkers, F. G. (**1994**). *Benign Lesions of the Vocal Folds: Clinical and Histopathological Aspects* (Drukkerij Van Denderen B. V., Groningen, The Netherlands).

Hess, M. M., Verdolini, K., Bierhals, W., Mansmann, U., and Gross, M. (**1998**). ''Endolaryngeal contact pressures,'' J. Voice **12**, 50–67.

Hirano, M., Kurita, S., and Nakashima, T. (**1983**). ''Growth, development and aging of human vocal folds,'' in *Vocal Fold Physiology; Contemporary Research and Clinical Issues*, edited by D. M. Bless and J. H. Abbs (College Hill, San Diego), pp. 23–43.

Holmberg, E. B., Hillman, R. E., and Perkell, J. S. (**1988**). ''Glottal air-flow and transglottal air-pressure measurements for male and female speakers in soft, normal, and loud voice,'' J. Acoust. Soc. Am. **84**, 511–529.

Ishizaka, K., and Flanagan, J. L. (**1972**). ''Synthesis of voiced sounds from a two-mass model of the vocal cords,'' Bell Syst. Tech. J. **51**, 1233–1268.

Jiang, J. J., Diaz, C. E., and Hanson, D. G. (**1998**). ''Finite element modeling of vocal fold vibration in normal phonation and hyperfunctional dysphonia: implications for the pathogenesis of vocal nodules,'' Ann. Otol. Rhinol. Laryngol. **107**, 603–610.

Jiang, J., Lin, E., and Hanson, D. G. (**2000**). ''Voice disorders and phonosurgery. I. Vocal fold physiology,'' Otolaryngol. Clin. North Am. **33**, 699–718.

Jiang, J. J., and Titze, I. R. (**1994**). ''Measurement of vocal fold intraglottal pressure and impact stress,'' J. Voice **8**, 132–144.

Kakita, Y., Hirano, M., and Ohmaru, K. (**1981**). ''Physical properties of vocal tissue: measurements on excised larynges,'' in *Vocal Fold Physiology*, edited by M. Hirano and K. Stevens (University of Tokyo Press, Tokyo), pp. 377–398.

Kaneko, T., Masuda, T., Akiki, S., Suzuki, H., Hayasaki, K., and Komatsu, K. (**1987**). ''Resonance characteristics of the human vocal fold *in vivo* and *in vitro* by an impulse excitation,'' in *Laryngeal Function in Phonation and Respiration*, edited by T. Baer, C. Sasaski, and K. S. Harris (Little, Brown, Boston), pp. 349–365.

Kuo, H.-K. J. (**1998**). ''Voice Source Modeling and Analysis of Speakers with Vocal-Fold Nodules,'' Ph.D. dissertation (Massachusetts Institute of Technology, Cambridge, MA), pp. 41–119.

Min, Y. B., Titze, I. R., and Alipour-Haghighi, F. (**1995**). ''Stress–strain response of the human vocal ligament,'' Ann. Otol. Rhinol. Laryngol. **104**, 563–569.

Story, B. H., and Titze, I. R. (**1995**). ''Voice simulation with a body-cover model of the vocal folds,'' J. Acoust. Soc. Am. **97**, 1249–1260.

Titze, I. R. (**1973**). ''The human vocal cords: A mathematical model. I,'' Phonetica **28**, 129–170.

Titze, I. R. (**1974**). ''The human vocal cords: A mathematical model. II,'' Phonetica **29**, 1–21.

Titze, I. R., and Strong, W. J. (**1975**). ''Normal modes in vocal cord tissues,'' J. Acoust. Soc. Am. **57**, 736–749.

Titze, I. R. (**1994**). ''Mechanical stress in phonation,'' J. Voice **8**, 99–105.

Titze, I. R., and Talkin, D. T. (**1979**). ''A theoretical study of the effects of various laryngeal configurations on the acoustics of phonation,'' J. Acoust. Soc. Am. **66**, 60–74.

Zeitels, S. M. (**1998**). ''Phonosurgery—past, present, and future,'' Operative Tech. Otolaryngol. Head Neck Surg. **9**, 179.

Zemlin, W. R. (**1998**). *Speech and Hearing Science: Anatomy and Physiology*, 4th ed. (Allyn and Bacon, Boston), pp. 137–152.